

# Radiation of Single Emitters Near Topological Insulators

24th AIP Congress

Eitan Dvorketz<sup>a</sup>, Benjamín Pavez<sup>a</sup>, Qiang Sun<sup>b,c</sup>, Andrew D. Greentree<sup>b,c</sup>,  
Brant C. Gibson<sup>b,c</sup>, Jerónimo R. Maze<sup>a</sup>

<sup>a</sup>Institute of Physics, Pontificia Universidad Católica de Chile, Santiago, Chile.

<sup>b</sup>School of Science, STEM College, RMIT University, Melbourne, VIC 3001, Australia.

<sup>c</sup>ARC Centre of Excellence for Nanoscale Biophotonics, RMIT University, Melbourne, VIC 3001, Australia.

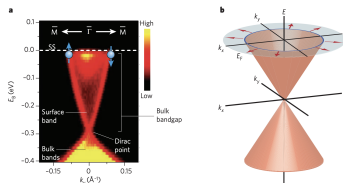
December 13, 2022



# Motivation

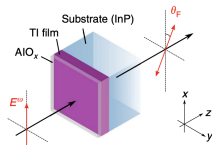
- Topological Insulators: Materials that present an insulating bulk while still having conductive edge states on their surface.
- Efforts to optically characterize TI seek to measure very small effects with specific and difficult-to-reproduce experimental conditions (i.e. Faraday Rotation).
- Objective: find new, fast, and spatially resolved techniques to characterize TIs optically.

## Dirac Cone for $\text{Bi}_2\text{Se}_3$ : ARPES vs Theoretical



Joel Moore. "The birth of topological insulators". In: *Nature* 464 (Mar. 2010), pp. 194–8

## Faraday Rotation on TI Setup Sketch



Ken N Okada et al. "Terahertz spectroscopy on Faraday and Kerr rotations in a quantum anomalous Hall state". In: *Nature communications* 7 (2016)

- 1 Lagrangian Characterization of Topological Insulators
  - Maxwell Equations for Topological Insulators
  - Boundary Conditions for TIs and Point Charge Example
- 2 Characterizing the Reflected Emissions
  - Fresnel Coefficients
- 3 Results
  - Addition of a third Mu-Metal Sublayer
  - Poynting Vector Analysis

# Lagrangian Characterization of Topological Insulators

# Maxwell Equations for Topological Insulators

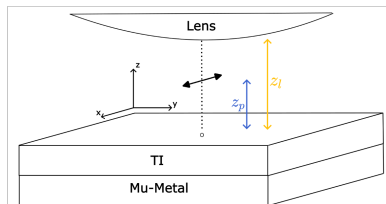
- The Lagrangian of TI is  $\mathcal{L}_0 + \mathcal{L}_{axion}$ , where  $\mathcal{L}_0$  is the usual electromagnetic Lagrangian and,

$$\mathcal{L}_{axion} = \frac{\alpha}{4\pi^2} \frac{\Theta(\mathbf{r}, \omega)}{\mu_0 c} \mathbf{E}(\mathbf{r}, \omega) \cdot \mathbf{B}(\mathbf{r}, \omega).$$

- This extra term changes the Maxwell equations introducing an electromagnetic coupling.
- The Helmholtz equation is, then,

$$\nabla \times \frac{1}{\mu(\mathbf{r}, \omega)} \nabla \times \mathbf{E}(\mathbf{r}, \omega) - \frac{\omega^2}{c^2} \epsilon(\mathbf{r}, \omega) \mathbf{E}(\mathbf{r}, \omega) - \frac{i\omega\alpha}{c\pi} [\nabla\Theta(\mathbf{r}, \omega) \times \mathbf{E}(\mathbf{r}, \omega)] = 0.$$

Sketch of Our Lens/Dipole/Material System



# Boundary Conditions for TIs and Point Charge Example

- The boundary conditions for a planar surface change.

$$[\hat{\mathbf{n}} \cdot \mathbf{B}]_{\Sigma} = 0,$$

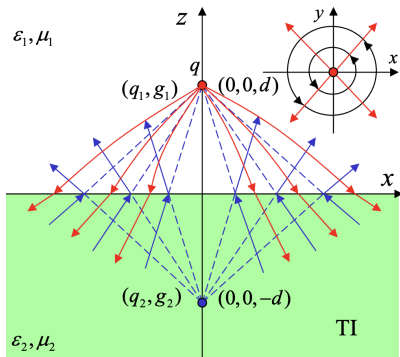
$$[\hat{\mathbf{n}} \times (\mathbf{B}/\mu)]_{\Sigma} = - \left( \frac{\alpha \Delta \Theta}{4\pi^2} \right) \hat{\mathbf{n}} \times \mathbf{E}|_{\Sigma},$$

$$[\hat{\mathbf{n}} \cdot \mathbf{E}]_{\Sigma} = 0,$$

$$[\hat{\mathbf{n}} \times (\epsilon \mathbf{E})]_{\Sigma} = - \left( \frac{\alpha \Delta \Theta}{4\pi^2} \right) \hat{\mathbf{n}} \cdot \mathbf{B}|_{\Sigma}.$$

- Point charge near TI's surface is a good example.

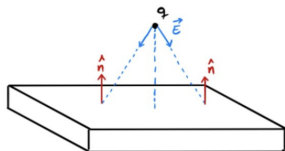
## Image Method Solution for Point Charge Near a TI



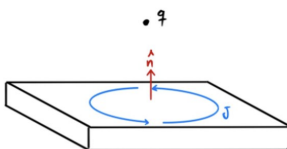
Xiao-Liang Qi et al. "Inducing a Magnetic Monopole with Topological Surface States". In: *Science* 323.5918 (2009), pp. 1184–1187

# Example: Point Charge near a Topological Insulator Surface

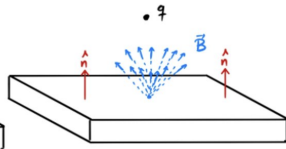
## Schematization of Topological Effects of a Point Charge Near a TI



$$\sigma_{xy} = \frac{\Theta}{2\pi} \frac{e^2}{h}$$



$$\mathbf{j} = \sigma_{xy} (\hat{\mathbf{n}} \times \mathbf{E})$$



$$\hat{\mathbf{n}} \times (\mathbf{B}/\mu) = \frac{\alpha}{\pi} \left( \frac{\Theta}{\sigma_{xy}} \right) \mathbf{j}$$

# Characterizing the Reflected Emissions



# Reflected and Transmitted Fields

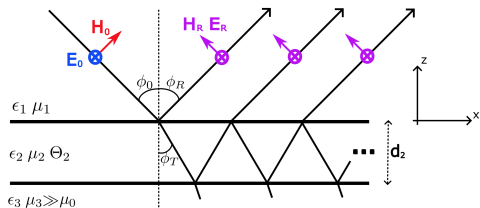
- Planar wave ansatz + new boundary conditions = Fresnel coefficients.
- New off-diagonal mixed coefficients appear:

$$\mathbf{R} = \begin{pmatrix} R_{TE,TE} & R_{TE,TM} \\ R_{TM,TE} & R_{TM,TM} \end{pmatrix}$$

- These new coefficients are small ( $\times 10^{-5}$ ) compared to the usual ones.

J. A. Crosse, Sebastian Fuchs, and Stefan Yoshi Buhmann. "Electromagnetic Green's function for layered topological insulators". In: *Phys. Rev. A* 92 (6 Dec. 2015), p. 063831

## TE polarized ray impacting the three-layered Air-TI-Mu-Metal system



# Adding a Third Mu-Metal Sublayer

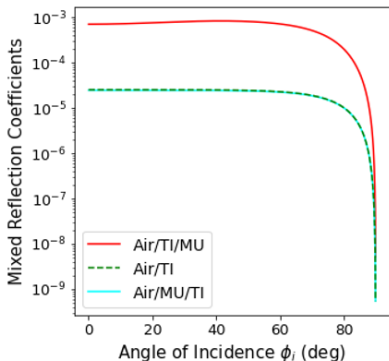


**Figure:** Mixed reflective coefficients as a function of the incidence angle for the three possible configurations.

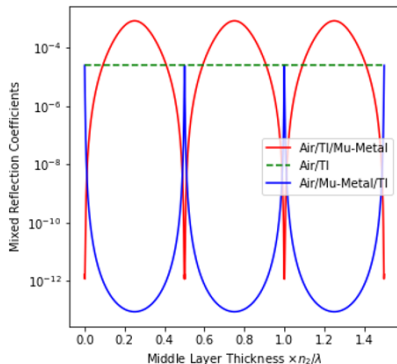


**Figure:** Mixed reflective coefficients as a function of the normalized middle layer's thickness.

# Electric Field Components

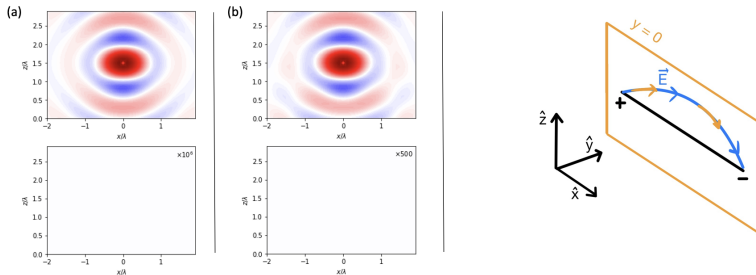


**Figure:** Electric field components  $\mathbf{E}_i \times \lambda$  of an  $\hat{x}$  oriented dipole, plotted in the  $y = 0$  plane, as a function of  $z/\lambda$  and  $x/\lambda$  for (a) free-space, (b) an Air/Magnetodielectric configuration, (c) an Air/TI configuration, and an Air/TI/Mu-Metal configuration.

# Electric Field Components

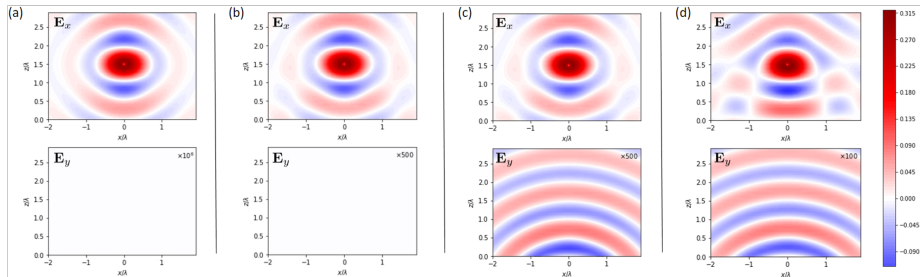


**Figure:** Electric field components  $\mathbf{E}_i \times \lambda$  of an  $\hat{x}$  oriented dipole, plotted in the  $y = 0$  plane, as a function of  $z/\lambda$  and  $x/\lambda$  for (a) free-space, (b) an Air/Magnetodielectric configuration, (c) an Air/TI configuration, and an Air/TI/Mu-Metal configuration.

# Poynting Vector Deviation

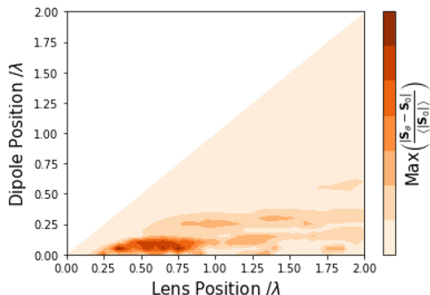


**Figure:** Maximum deviation in the  $\hat{y}$  axis of the Poynting vector for a set of collection lens-dipole-TI configurations.

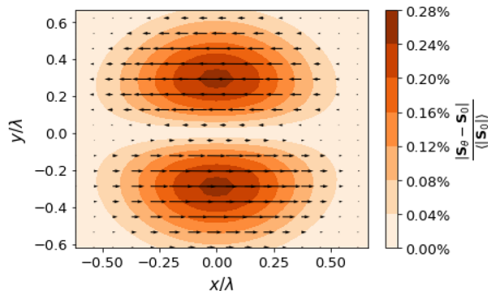
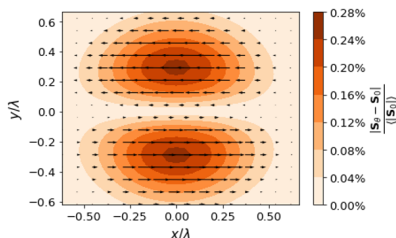
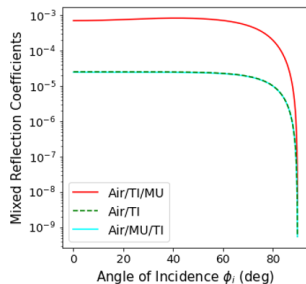


**Figure:** Difference between the Poynting vector generated by an  $\hat{x}$  oriented dipole over a TI's surface  $\mathbf{S}_\theta$ , and over the equivalent magnetodielectric surface  $\mathbf{S}_0$ .

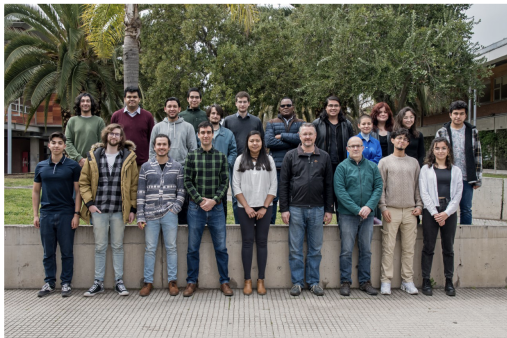
# Summary

- By adding a third Mu-Metal sub-layer, we predict an increase of  $\sim \times 10^2$  for a TI with impedance  $Z = \sqrt{2}$ .
- We were able to pinpoint the optimal TI middle layer's thickness, given its optical characteristics.
- We theorized a far-field Poynting vector deviation of 0.28% with an optimal system configuration, for a room temperature TI.
- Future prospects: Quantum analysis and NV-center characterization.



# Acknowledgments

- We acknowledge the support from the Air Force Office of Scientific Research (AFOSR) FA2386-21-1-4125, Fondecyt Regular No 1221512, and Anillo ACT192023 for this work.



Quantum Optics team Pontificia Universidad Católica de Chile (PUC)

